INVESTIGATION ON 3-D STRUCTURE IN SIDE-CAVITY OPEN-CHANNEL FLOW BY LES

Kouki Onitsuka
Department of Civil Engineering, Kyushu Institute of Technology
Kita-Kyushu, 804-8550, Japan
onitsuka@civil.kyutech.ac.jp

Masaru Ura
Hinosato 9-5-5, Munakata, Fukuoka 811-3425, Japan

Juichiro Akiyama
Department of Civil Engineering, Kyushu Institute of Technology
Kita-Kyushu, 804-8550, Japan
juichiro@tobata.isc.kyutech.ac.jp

Iehisa Nezu
Department of Civil and Global Environment Engineering, Kyoto University
Kyoto, 606-8501, Japan
nezu@nezu.gee.kyoto-u.ac.jp

ABSTRACT

A numerical simulation of an open-channel flow with a side cavity has been carried out by making use of an LES (large eddy simulation). In this study, the Froude number was set to 0.1, based on the study by Kimura *et al.*(1997), that the fluctuations of free surface are negligibly small in such a low Froude number flow. The time-averaged velocity vector, distributions of the Reynolds stress and kinetic turbulent energy are similar to those of experimental data which were obtained by Nezu & Onitsuka(2001) with an LDA (laser Doppler anemometer). It was found that the instantaneous velocity vector is quite different from the time-averaged one. The calculated flow field is almost 2-dimensional in the vertical direction except for very near the bed. This result corresponds to the experimental data which was shown by Nezu et al.(2000) with a PIV (particle image velocimetry) It was found that the weak up-flow was generated at the central pivot of the time-averaged horizontal vortex and that the shape and the strength of the instantaneous horizontal vortex in the same time change in the vertical direction.

INTRODUCTION

Recently, the side-cavity has gathered great public attentions from a point of view not only in river engineering but also in water environment, because the side-cavity offers a comfortable environment to aquatic animals and plants as well as human beings in eco-systems. At present, some artificiality side-cavity has been constructed in the rivers for the purpose of the maintenance of the river environment. Therefore it is quite important to investigate such flows.

Coherent horizontal vortices are generated by the Kelvin-Helmholtz instability between the main channel and the side-cavity. Mass and momentum are transported between the side-cavity and the main channel by not only the time-averaged velocity but also the instantaneous velocity fluctuations, so that the investigation of the 3-D structure in the side-cavity open-channel flows are quite important. Chen & Ikeda(1996) and Ikeda et al.(1999) have shown that the frequency of horizontal vortices decreases along the downstream, because some vortices coalesce with each other and their spatial scale increases in the downstream direction. Muto et al.(2000) have measured the velocities in two cases of the side-cavity open-channel flows with an LDA (laser Doppler anemometer) and flow visualization techniques. They have indicated that the momentum transfer from the main-channel toward the side-cavity is lager than that from the side-cavity toward the main-channel. Nezu et al.(2000) and Nezu & Onitsuka(2001) have measured instantaneous velocity fields in and around the side-cavity at the middle depth with the aspect ratio of 2, 3, 5 and 10 by making use of PIV and LDA. They clarified the process of development of vortex that is generated in the side-cavity by the shear instability.

As mentioned the above, some experimental investigations on turbulent structure about the side-cavity open-channel flows have been conducted. Almost investigation is on the vortex which generated by the shear instability in spanwise direction. The shear is also generated by not only the shear between the side-cavity and main channel but also the side and bed wall, so that it is necessary to analyze 3-D instantaneous velocity data in order to investigate 3-D coherent structure in the

Table-1 Hydraulic Condition

	L cm	B_w cm	B cm	Fr	Re $\times 10^3$
LDA (Nezu & Onitsuka)	20	4.0	35.0	0.49	12
PIV (Nezu et al.)					
LES (present study)			16.0	0.1	2.5

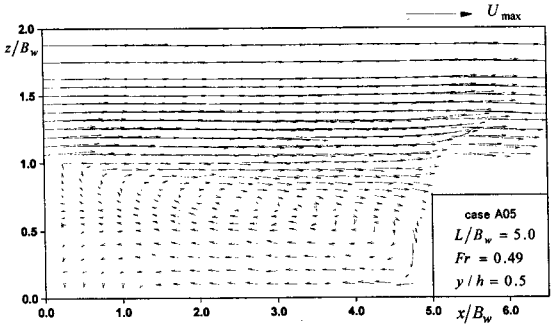

Fig.1(a) Time-averaged flow vector (U , W) (LDA)

side-cavity. In spite of many researchers' efforts, almost all experimental data are only 1-D and 2-D, due to difficulty of obtaining 3-D instantaneous data from experiments. In contrast, it is comparably easy to obtain such data from the 3-D numerical simulation such as an LES (Large Eddy Simulation) and DNS (Direct Numerical Simulation). It is easy to investigate all instantaneous velocities in the same time on the basis of the LES data. Recently, some simulations of uniform and wavy shaped open-channel flows have been conducted by making use of LES and DNS. However, there is little investigation on the side-cavity open-channel flow by LES. In this study, a numerical simulation by LES has been conducted to investigate 3-D coherent structure in the side-cavity open-channel flow.

NUMERICAL METHOD

The filtered continuity equation and N-S equation are described as follows:

$$\frac{\partial \overline{u_i}}{\partial x_i} = 0 \tag{1}$$

$$\frac{\partial \overline{u_i}}{\partial t} + \frac{\partial \left(\overline{u_i}\,\overline{u_j}\right)}{\partial x_j} = F_i - \frac{\partial}{\partial x_i}\left(\frac{\overline{p}}{\rho} + \frac{2}{3}k\right) + \nu \frac{\partial^2 \overline{u_i}}{\partial x_j^{\,2}} - \frac{\partial \tau_{ij}}{\partial x_j} \tag{2}$$

$$\tau_{ij} \equiv \overline{u_i u_j} - \overline{u_i}\,\overline{u_j} \tag{3}$$

$$F_i = \left(g\sin\theta, -g\cos\theta, 0\right) \tag{4}$$

in which the over bar $\overline{\ }$ denotes the faltered value, $\overline{u_i}$ is the velocity component in the i direction (i=1,2,3). x_1 is the streamwise direction, x_2 is the vertical direction and x_3 is the spanwise ones. $\overline{p}$ is the filtered pressure, $k \equiv \overline{u_i' u_j'}/2$ is the turbulent kinetic energy of SGS (Sub-Grid Scale). The SGS stress tensor τ_{ij} is defined as follows:

$$\tau_{ij} = \nu_t \left(\frac{\partial \overline{u_i}}{\partial x_j} + \frac{\partial \overline{u_j}}{\partial x_i}\right) \tag{5}$$

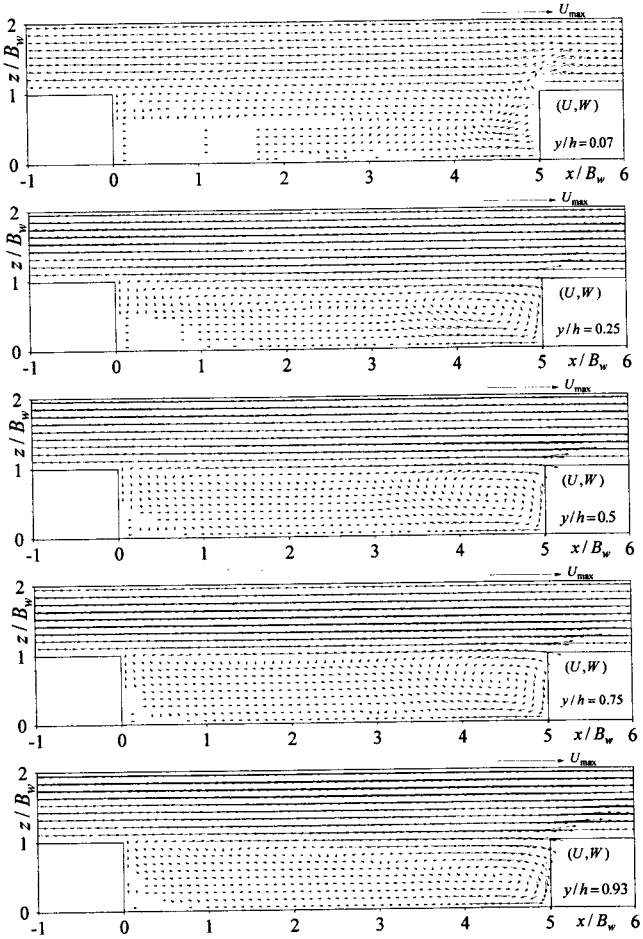

Fig.1(b) Time-averaged flow vector (U , W) (LES)

as the SGS eddy viscosity ν_t. The following 1-equation model was adapted,

$$\frac{\partial k}{\partial t} + \overline{u}_j \frac{\partial k}{\partial x_j} = 2\nu_t \overline{D}^2 - C_\varepsilon \frac{k^{2/3}}{\Delta} + \frac{\partial}{\partial x_j}\left\{\left(\frac{\nu_t}{\sigma_k} + \nu\right)\frac{\partial k}{\partial x_j}\right\} \tag{6}$$

$$D_{ij} \equiv \frac{1}{2}\left(\frac{\partial u_i}{\partial x_j} + \frac{\partial u_j}{\partial x_i}\right) \tag{7}$$

$$\overline{D} = \left(\overline{D}_{ij}\overline{D}_{ij}\right)^{1/2} \tag{8}$$

$$\nu_t = C_\nu \Delta k^{1/2} \tag{9}$$

$$\Delta = \left(\Delta_1 \Delta_2 \Delta_3\right)^{1/3} \tag{10}$$

The model constants are chosen as C_ν=0.1, σ_k=0.5, C_ε=1.0 of the Nezu & Yamamoto(1998).

The second-order centered difference scheme was used for spatial differentiation and second-order Adams-Bashforth method was adopted for time differentiation. The Poisson equation for solving the pressure was calculated by using the conjugate residual method.

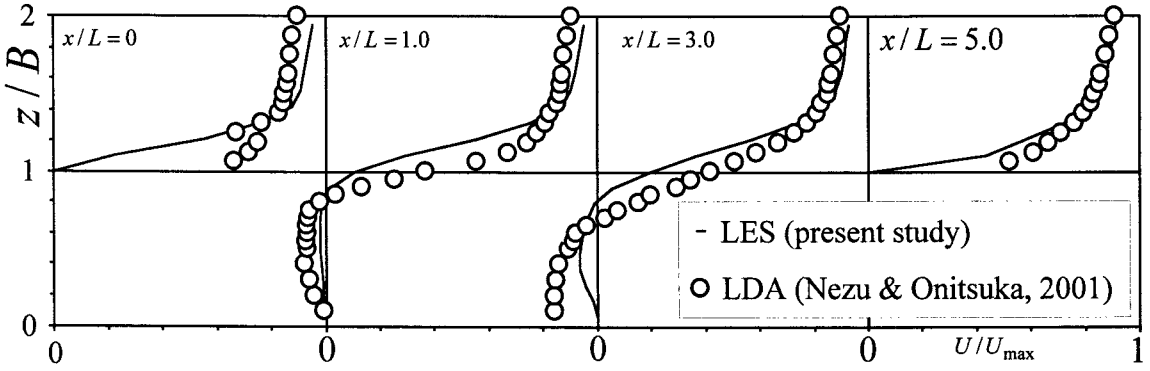

Fig.2 variation of the profiles of the time-averaged velocity (U) to the downstream direction

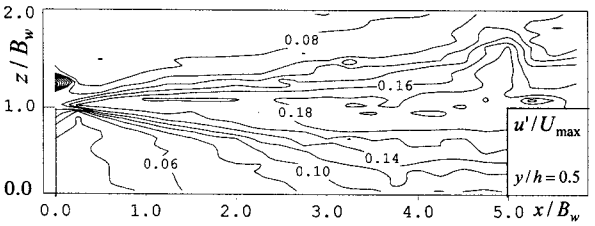

Fig.3(a) Turbulence Intensity of Streamwise Component $u'/U_{\max}$ (LDA)

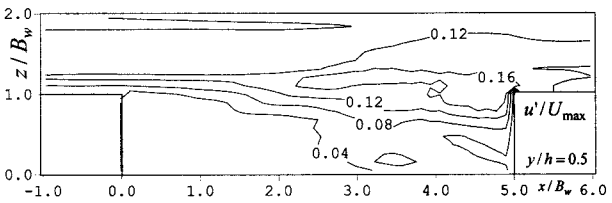

Fig.3(b) Turbulence Intensity of Streamwise Component $u'/U_{\max}$ (LES)

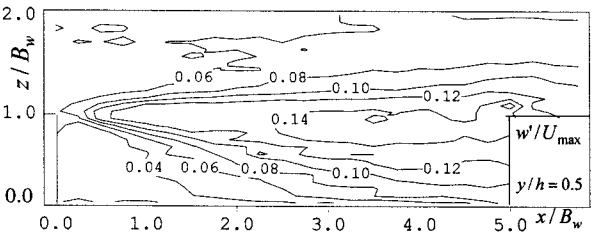

Fig.4(a) Turbulence Intensity of Spanwise Component $w'/U_{\max}$ (LDA)

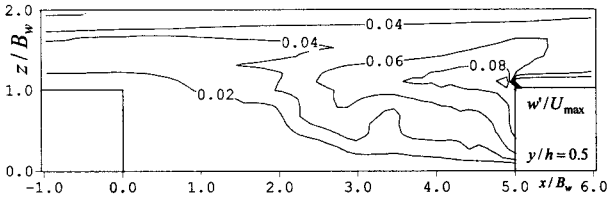

Fig.4(b) Turbulence Intensity of Spanwise Component $w'/U_{\max}$ (LES)

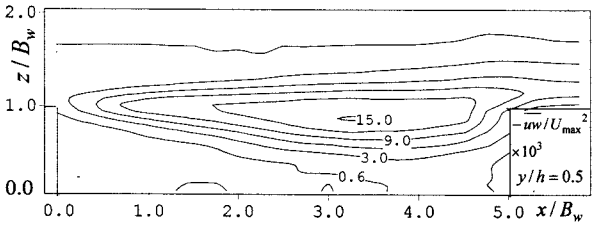

Fig.5(a) Spanwise Reynolds Stress $-\overline{uw}/U_{\max}{}^2$ (LDA)

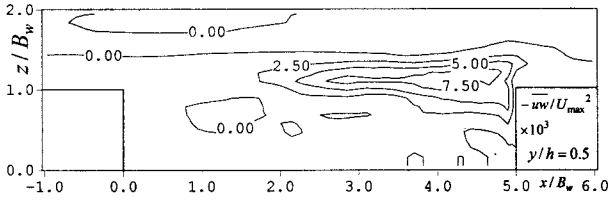

Fig.5(b) Spanwise Reynolds Stress $-\overline{uw}/U_{\max}{}^2$ (LES)

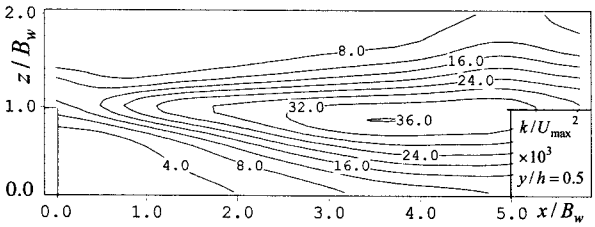

Fig.6(a) Kinetic Turbulent Energy $k/U_{\max}{}^2$ (LDA))

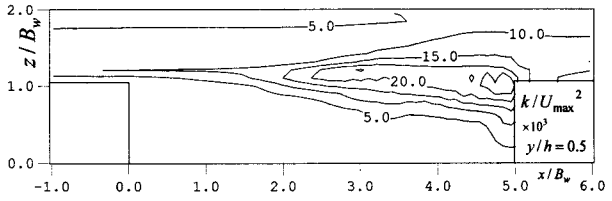

Fig.6(b) Kinetic Turbulent Energy $k/U_{\max}{}^2$ (LES)

HYDRAULIC CONDITION

The hydraulic condition for the calculation is given in Table-1, together with that of Nezu et al.(2000) and Nezu & Onitsuka's(2001) experiments. h is the flow depth, B is the channel width, $Fr \equiv U_m / \sqrt{gh}$ is the Froude number and U_m is the bulk mean velocity. The aspect ratio (streamwise length of the side-cavity / spanwise length of the side-cavity) and the flow depth of the calculation are the same as those of experiments. But the channel width and Froude number are changed, due to the memory capacity of the computer. As a result, the Reynolds number of the calculation is also different from that of the experiment.

x, y and z are streamwise, vertical and spanwise axis, respectively. u', v' and w' are the turbulence

intensity of the x, y and z component and U, V and W are the time averaged velocity components. Number of computational grid was chosen as 200, 15 and 40 for x, y and z directions, respectively. As a result, the cell sizes in a wall unit are $\Delta x^+ \equiv \Delta x U_* / \nu$ =13.1, Δy =8.3 and Δz =13.1. The streamwise length at the upstream reach of the side-cavity is 0.8 L and that at the downstream reach of the side-cavity is 2.2 L. The boundary conditions are as follows; the non-slip at the side and bed walls, v =0 and u and w are the zero gradient condition at the free surface, the cyclic boundary conditions at the entrance and exit of the calculating volume. The turbulence statistics were calculated during 10,000 time steps after 600,000 time steps.

RESULTS AND DISCUSSION

Velocity Vectors in Horizontal Planes

Fig.1(a) shows the time-averaged velocity vectors (U, W) at the middle depth (y/h =0.5) normalized by the maxim streamwise velocity U_{max} at the inlet of the side-cavity (x =0) measured by Nezu & Onitsuka(2001). Fig.1(b) shows the time-averaged velocity vectors (U, W) at several vertical position calculated in the present study. At the middle depth (y/h =0.5), a horizontal vortex is observed both of calculation and experiment. The pattern of the horizontal vortex obtained from the calculation is similar to that obtained from the experiment. The scale of the vortex of calculation is smaller than that of experiment. This maybe caused by the differences of the Reynolds and Froude number between the calculation and experiment.

Nezu et al.(2000) have measured horizontal vortices at y/h =0.25, 0.5 and 0.75 with PIV in the case of the aspect ratio of 2, and found that the time-averaged velocities are constant in the vertical direction in the range of $0.25 \leq y/h \leq 0.75$. The calculated results show that the flow field are similar in the vertical direction except for the very near the free surface and the bed. This tendency corresponds well to Nezu et al.(2000)'s experimental result. In contrast, the location of the central pivot of the horizontal vortex near the free surface is different from that at the middle depth. The flow pattern near the bed is quite different from other planes. Therefore, the time-averaged flow fields are 2-dimensional in the vertical direction except for near the free surface and near the bed.

Fig.2 shows the variation of the profiles of the time-averaged velocity (U) to the downstream direction (x/L =0, 1.0, 3.0, 5.0). The line means the LES results and the plot means the LDA data obtained by Nezu & Onitsuka(2001). The velocity of LDA data takes negative value near the side-wall inside of the side-cavity. Although, there is some deference, the LES data is in a good agreements with LDA data.

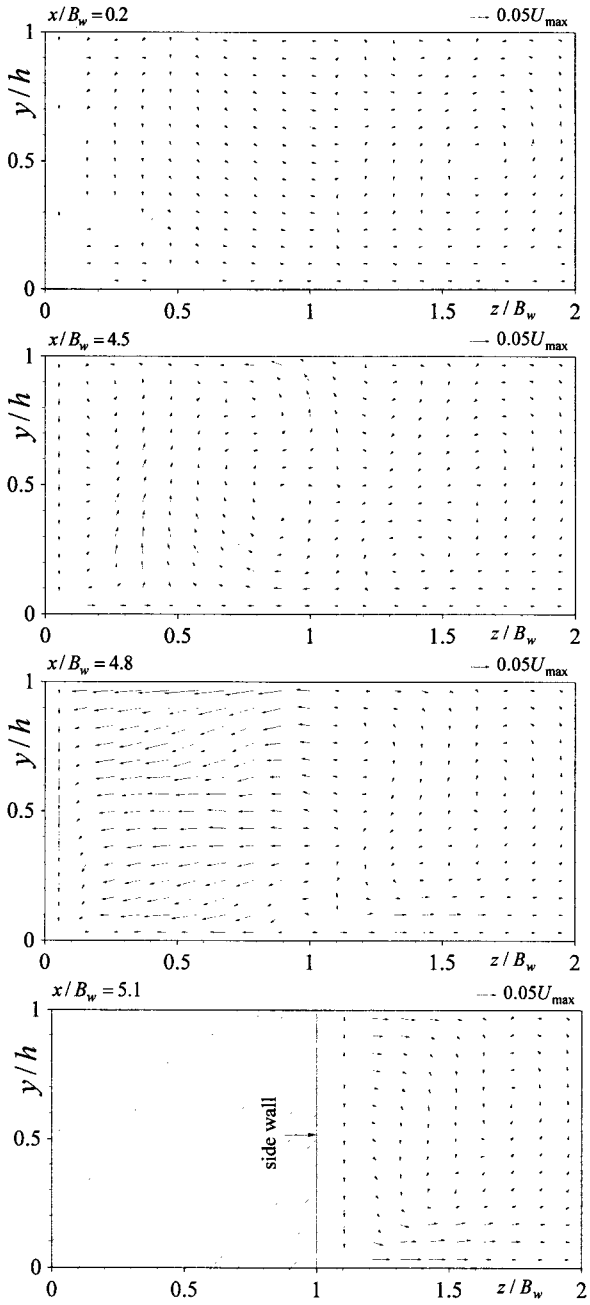

Fig.7 Secondary Currents in Cross Section (LES)

Turbulent Characteristics in Horizontal Planes

Figs.3 and 4 show the contour lines of the turbulence intensity u' and w' at the middle depth (y/h =0.5) normalized by the U_{max}, respectively. The strength of u'/U_{max} and w'/U_{max} increases in the downstream direction at the interface between side-cavity and the main channel in both figures. The pattern of the u'/U_{max} obtained from the calculation is similar to that obtained from the experiment. Although, the values of u'/U_{max} and w'/U_{max} are different from each other. This maybe due to the Reynolds and Froude number differences.

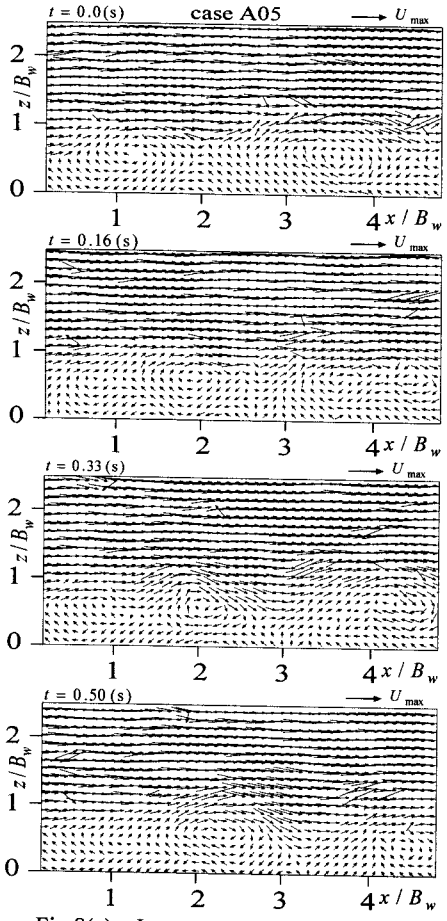

Fig.8(a) Instantaneous Velocity Vectors in Horizontal Plane (LDA)

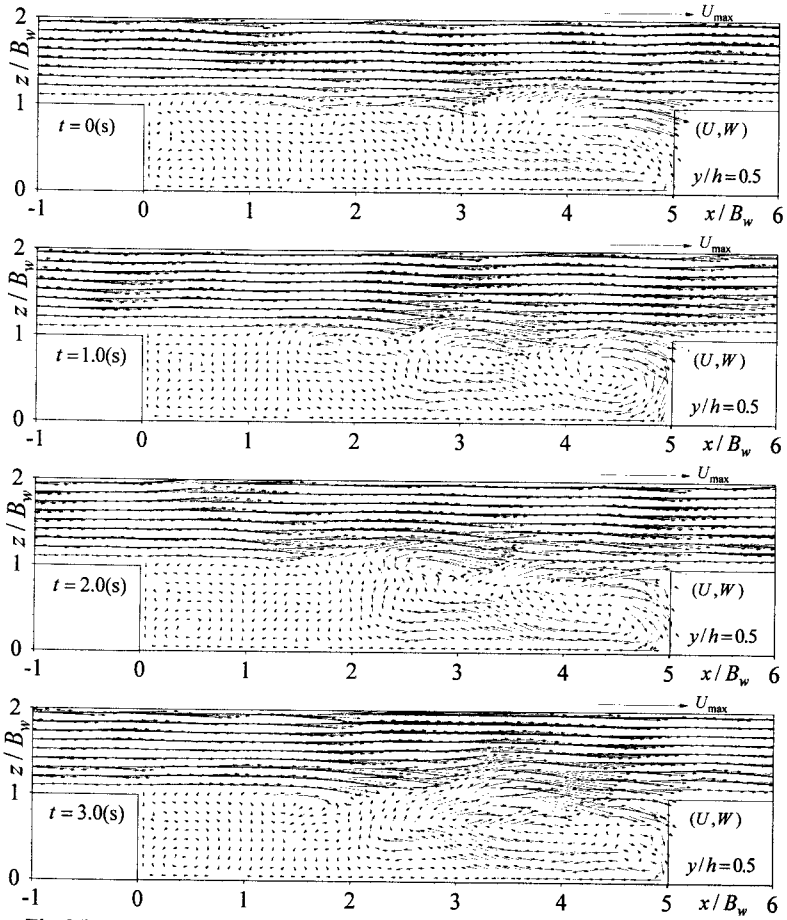

Fig.8(b) Instantaneous Velocity Vectors in Horizontal Plane (LES)

Figs.5(a) and (b) show the contour lines of the spanwise Reynolds stress $-\overline{uw}$ at the middle depth (y/h =0.5) normalized by U_{max} obtained from the experiment and calculation, respectively. It can be seen that the spanwise width of the shear layer increases in the downstream direction both of experiment and calculation.

In calculation, all three components of the turbulent fluctuations can be obtained. Consequently, the kinetic turbulent energy k can be obtained by the following equation:

$$k \equiv (u'^2+v'^2+w'^2)/2 \qquad (11)$$

On the other hand, Nezu & Onitsuka(2001) have measured only the streamwise and spanwise velocity components with a 2-dimensional LDA system. The kinetic turbulent energy k in the case of experiment is calculated approximately as follows (see Nezu & Nakagawa, 1993):

$$k \approx (u'^2+2w'^2)/2 \qquad (12)$$

Figs.6(a) and (b) show the contour lines of the kinetic turbulent energy k at the middle depth (y/h =0.5) normalized by U_{max} obtained from the experiment and calculation, respectively. The maximum values of k both of calculation and experiment are located a little downstream position from the position of the maximum spanwise Reynolds stress. This maybe because the turbulent generation rate is larger than the turbulent dissipation rate at the area where is enclosed area by the maximum Reynolds stress position and the maximum kinetic turbulent energy one.

Development of Horizontal Vortex

Figs.7(a) and (b) show the instantaneous velocity vector ($\tilde{u}$, $\tilde{w}$) in the horizontal plane at the middle depth (y/h =0.5) obtained from the experiment and calculation, respectively. Nezu et al.(2000) have pointed out that the horizontal vortex is generated at the interface (z/B_w =1.0) and traveling toward the downstream direction with increasing its scale in the case that the aspect ratio is 5. Such a phenomenon is also observed in the calculated flow fields. It is seen from the Fig.7(b) that the scale of the horizontal vortex increases in the downstream, due to the vortex entrains the surrounding water. The velocity fluctuations at the upstream area inside of the side-cavity ($0< x/B_w <2.0$) are very small in comparison with those at the downstream area. This situation is also corresponding to that of experiment.

Secondary Currents in Cross Section

Fig.8 shows the secondary currents in the several cross sections. The strength of the secondary currents at x/B_w =0.2 is less than 1% of the time-averaged streamwise velocity. In contrast, an up-current is seen at x/B_w =4.5. The strength of this up-current is 3% of the time-averaged streamwise velocity. The center of the up-current is located at $0.4< z/B_w <0.5$. This position is

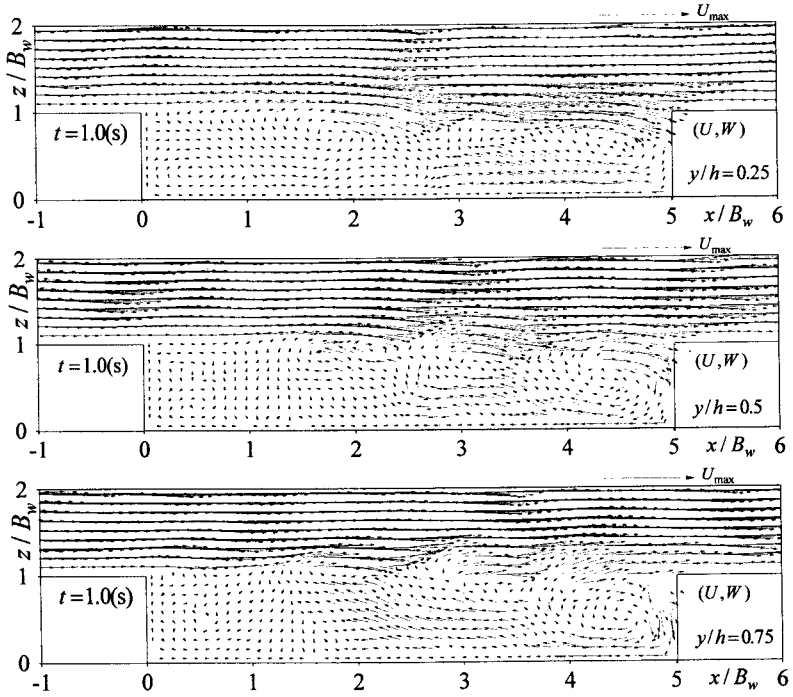

Fig.9 Instantaneous Velocity Vectors in Horizontal Planes at Several Positions (LES)

corresponding to that of the central pivot of the time-averaged horizontal vortex (see Fig.1). Experimental result of the up-current in the side-cavity open-channel flows have not been reported. It is necessary to investigate the up-current by the experiments.

Variation of Horizontal Vortex in Vertical Direction

Fig.9 shows the instantaneous velocity vector ($\tilde{u}$, $\tilde{w}$) in the horizontal planes at several vertical positions (y/h =0.25, 0.5, 0.75) in the same time obtained from the calculation. There is no experimental data corresponding to Fig.7, because it is quite difficult to obtain such instantaneous velocities from the experiment. The scale and strength of the horizontal vortex changes in the vertical direction slightly. The position of the central pivot of the vortex also changes in the vertical direction.

CONCLUDED REMARKS

A numerical simulation of an open-channel flow with a side-cavity was carried out by a large eddy simulation (LES) involved with one-equation model. The calculated time-averaged statistics such as the velocity distribution in the horizontal plane and the spanwise Reynolds stress at the middle depth are in a good agreement with experimental data, which was obtained by Nezu et al.(2000) and Nezu & Onitsuka(2001) with LDA and PIV. The weak up-flow was observed at the central pivot of the horizontal vortex. The shape and strength of the horizontal vortex in the same time change in the vertical direction.

ACKNOWLEDGEMENT

This work was supported by Grant-in-Aid for Encouragement of Young Scientists (Project No.14750427, Head Investigator: K. Onitsuka) of The Ministry of Education, Culture, Sports, Science and Technology of Japan.

REFERENCES

Chen, F. and Ikeda, S., 1996, " Experimental study on horizontal separation eddies in open-channel flow with groins", Ann. J. of Hydraulic Eng., JSCE, Vol.40, 787 (in Japanese).

Ikeda, S., Yoshike, T. and Sugimoto, T., 1999, "Experimental study on the structure of open channel flow with impermeable spur dikes", Annual J. of Hydraulic Eng., JSCE, Vol.43, 281 (in Japanese).

Kimura, I., Hosoda, T, Yasunaga, R. and Muramoto, Y., 1997, "Characteristics of fluid oscillation around a dead zone in open channel flows", Annual J. of Hydraulic Eng., JSCE, Vol.41, 711 (in Japanese).

Muto, Y., Imamoto, H. and Ishigaki, T., 2000, "Velocity measurements in a straight open channel with a rectangular embayment", Proc. of 12th Cong. of APD-IAHR, Bangkok, Thailand, 353.

Nezu, I., Onitsuka, K., Iketani, K. and Takahashi, S., 2000, " Turbulence characteristics of side-cavity "Wando" open-channel flows", Proc. of 12th Cong. of APD-IAHR, Bangkok, Thailand, 21.

Nezu, I. and Onitsuka, K., 2001, "LDA measurements of side-cavity "Wando" open-channel flows" Proc. of 8th Int. Symp. on Flow Modeling and Turbulence Measurements, Tokyo, Japan, 83.

Nezu, I. and Yamamoto, Y., 1998, 7th Int. Symp. on Flow Modeling and Turbulence Measurements, Tainan, Taiwan, pp.381-390.

Nezu, I. and Nakagawa, H., 1993, "*Turbulence in Open-Channel Flows*", IAHR-Monograph, Belkema, Netherlands.